Journal of Geophysical Research: Atmospheres

Supporting Information for

Wildfire Smoke Influence on Cloud Water Chemical Composition at Whiteface Mountain, New York

Jamy Y. Lee[1], Peter K. Peterson[1†], Logan R. Vear[1], Ryan D. Cook[1], Amy P. Sullivan[2], Ellie Smith[3], Lelia N. Hawkins[3], Nicole E. Olson[1], Rachel Hems[1], Philip K. Snyder[4], Kerri A. Pratt[1,5*]

[1]Department of Chemistry, University of Michigan, Ann Arbor, MI, USA
[2]Department of Atmospheric Science, Colorado State University, Fort Collins, CO, USA
[3]Department of Chemistry, Harvey Mudd College, Claremont, CA, USA
[4]Adirondack Lake Survey Corporation, Ray Brook, NY, USA
[5]Department of Earth and Environmental Sciences, University of Michigan, Ann Arbor, MI, USA
†Now at the Department of Chemistry, Whittier College, Whittier, CA, USA

*Corresponding author: Kerri A. Pratt (prattka@umich.edu)

Contents of this file

Text S1
Figures S1 to S4
Tables S1 to S3

Text S1. Additional Discussion on Dissolved Organic Carbon Concentrations

Succinic acid, a highly water-soluble dicarboxylic acid, is emitted from biomass burning (Zhao et al., 2014), vehicular combustion (Thepnuan et al., 2019), and formed in the photooxidation of fatty acids (Kawamura & Gagosian, 1987). Further, particle-phase succinate increases in concentration with atmospheric aging (Gao et al., 2003). Succinate concentrations were greatest in samples C1 and C4, which were influenced by urban emissions when the air masses were below the boundary layer (**Table S2**). Thus, the increase in succinate concentrations for these two samples were likely influenced by urban emissions, in addition to smoke.

Formic and acetic acid are directly emitted from biomass burning (Yu, 2000), with high formic:acetic acid mass ratios (1.2 – 1.9) indicating additional secondary formation of formic acid within cloud droplets (Li et al., 2020). Formate and acetate were detected in all cloud water case samples (formate:acetate ratios of 0.4 – 1.3); however, there are multiple sources and sinks of aqueous formate and acetate (Paulot et al., 2011).

Concentrations of methanesulfonic acid (MSA) produced from the oxidation of dimethylsulfide and dimethyl sulfoxide (Yuan et al., 2004) have been observed to be enhanced in biomass burning influenced cloud water (Stahl et al., 2021). MSA can also be sourced from oceanic emissions (Yuan et al., 2004), anthropogenic emissions (Yuan et al., 2004), and urban and feedlot areas (Sorooshian et al., 2015).

Glycerol was one of the top five most abundant carbohydrate measured for all five case samples (**Table S3**). The percentage of glycerol to TOC ranged from 4 – 70% for all five case samples (**Table S3**). Glycerol was enhanced in samples with higher levoglucosan concentrations (C3 and C5), as previously observed by Urban et al. (2014) for atmospheric particles in Brazil.

References.

Gao, S., Hegg, D. A., Hobbs, P. V., Kirchstetter, T. W., Magi, B. I., & Sadilek, M. (2003). Water-soluble organic components in aerosols associated with savanna fires in southern Africa: Identification, evolution, and distribution. *Journal of Geophysical Research: Atmospheres, 108*(D13). https://doi.org/10.1029/2002JD002324. https://doi.org/10.1029/2002JD002324

Kawamura, K., & Gagosian, R. B. (1987). Implications of ω-oxocarboxylic acids in the remote marine atmosphere for photo-oxidation of unsaturated fatty acids. *Nature, 325*(6102), 330-332. https://doi.org/10.1038/325330a0

Li, T., Wang, Z., Wang, Y., Wu, C., Liang, Y., Xia, M., et al. (2020). Chemical characteristics of cloud water and the impacts on aerosol properties at a subtropical mountain site in Hong Kong SAR. *Atmos. Chem. Phys., 20*(1), 391-407. https://acp.copernicus.org/articles/20/391/2020/

Paulot, F., Wunch, D., Crounse, J. D., Toon, G. C., Millet, D. B., DeCarlo, P. F., et al. (2011). Importance of secondary sources in the atmospheric budgets of formic and acetic acids. *Atmos. Chem. Phys., 11*(5), 1989-2013. https://acp.copernicus.org/articles/11/1989/2011/

Sorooshian, A., Crosbie, E., Maudlin, L. C., Youn, J.-S., Wang, Z., Shingler, T., et al. (2015). Surface and airborne measurements of organosulfur and methanesulfonate over the western United States and coastal areas. *Journal of Geophysical Research: Atmospheres, 120*(16), 8535-8548. https://doi.org/10.1002/2015JD023822. https://doi.org/10.1002/2015JD023822

Stahl, C., Crosbie, E., Bañaga, P. A., Betito, G., Braun, R. A., Cainglet, Z. M., et al. (2021). Total organic carbon and the contribution from speciated organics in cloud water: airborne data analysis from the CAMP2Ex field campaign. *Atmos. Chem. Phys., 21*(18), 14109-14129. https://acp.copernicus.org/articles/21/14109/2021/

Thepnuan, D., Chantara, S., Lee, C.-T., Lin, N.-H., & Tsai, Y. I. (2019). Molecular markers for biomass burning associated with the characterization of PM2.5 and component sources during dry season haze episodes in Upper South East Asia. *Science of The Total Environment, 658*, 708-722. https://www.sciencedirect.com/science/article/pii/S0048969718350642

Urban, R. C., Alves, C. A., Allen, A. G., Cardoso, A. A., Queiroz, M. E. C., & Campos, M. L. A. M. (2014). Sugar markers in aerosol particles from an agro-industrial region in Brazil. *Atmospheric Environment, 90*, 106-112. https://www.sciencedirect.com/science/article/pii/S135223101400209X

Yu, S. (2000). Role of organic acids (formic, acetic, pyruvic and oxalic) in the formation of cloud condensation nuclei (CCN): a review. *Atmospheric Research, 53*(4), 185-217. https://www.sciencedirect.com/science/article/pii/S0169809500000375

Yuan, H., Wang, Y., & Zhuang, G. (2004). MSA in Beijing aerosol. *Chinese Science Bulletin, 49*(10), 1020-1025. https://doi.org/10.1007/BF03184031

Zhao, R., Mungall, E. L., Lee, A. K. Y., Aljawhary, D., & Abbatt, J. P. D. (2014). Aqueous-phase photooxidation of levoglucosan - a mechanistic study using aerosol time-of-flight chemical ionization mass spectrometry (Aerosol ToF-

CIMS). *Atmos. Chem. Phys., 14*(18), 9695-9706. https://acp.copernicus.org/articles/14/9695/2014/

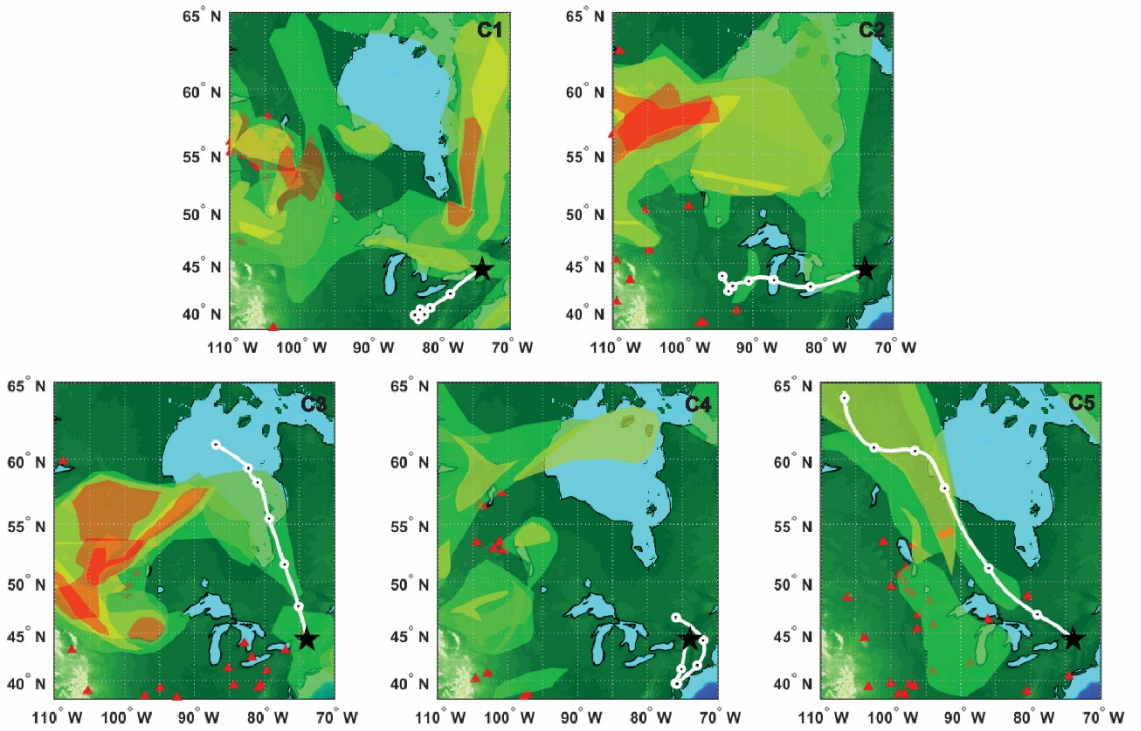


Figure S1. Type Air mass trajectories and smoke/fire maps for Whiteface Mountain cloud water case study samples, as defined in Table S2. NOAA HYSPLIT 72 h backward air mass trajectories (white lines, with black dots representing every 12 h resolution) are overlaid on smoke maps, where green, yellow, and red shading indicates thin, medium, and thick amounts of smoke, respectively, as defined by the NOAA HMS Fire and Smoke Product. Red triangles indicate locations of satellite-detected wildfires. Case study sample labels are listed in the top right corner of each smoke map.

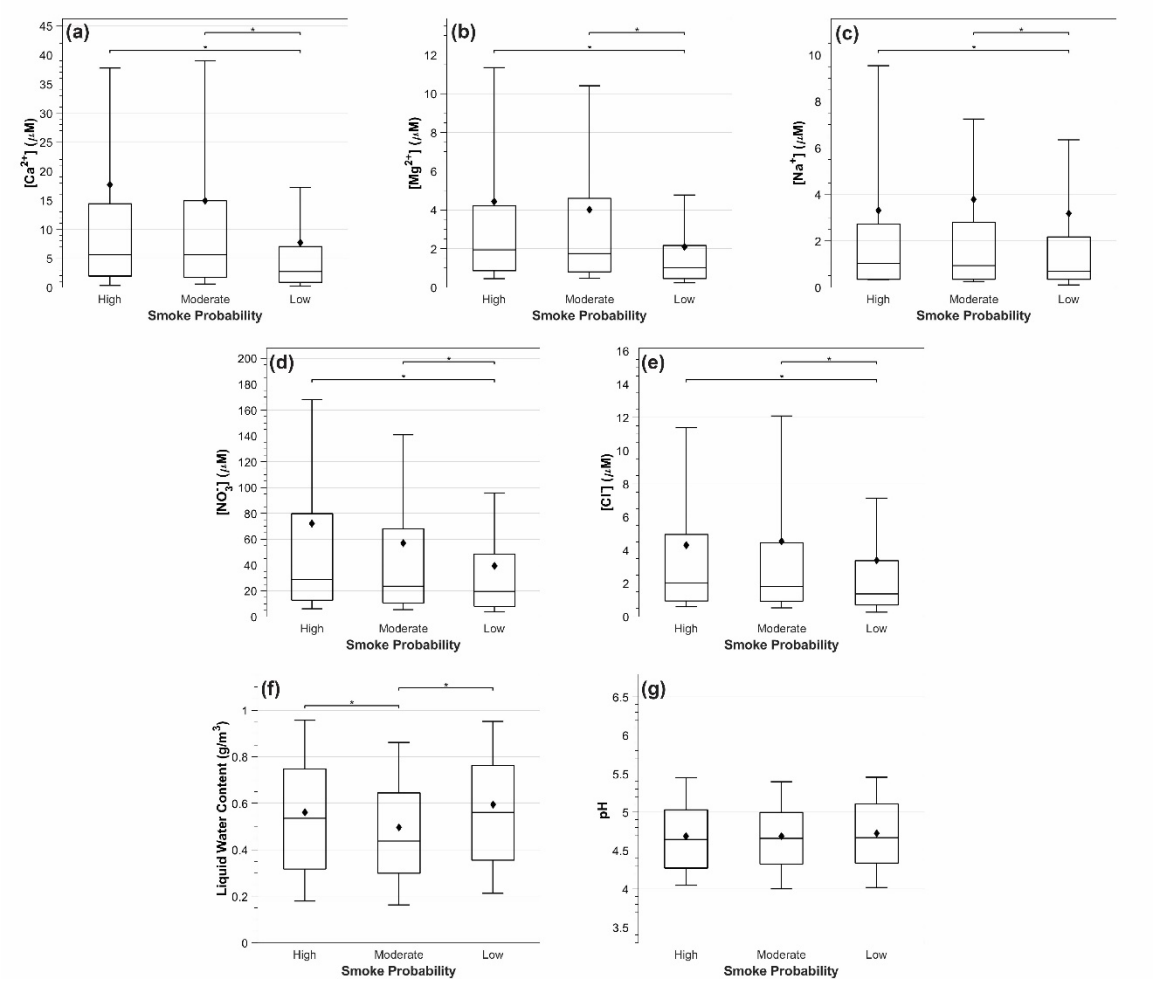


Figure S2. Boxplot distributions for cloud water concentrations of (a) calcium (Ca^{2+}), (b) magnesium (Mg^{2+}), (c) sodium (Na^{+}), (d) nitrate (NO_3^{-}), (e) chloride (Cl^{-}), (f) liquid water content, and (g) pH per category of smoke influence probability (high, moderate, and low). Boxplots represent the 25th, 50th, and 75th percentiles with whiskers representing the 10th and 90th percentiles. Average concentrations per category are marked as diamonds. Significant differences in the distributions that met both the Kruskal-Wallis non-parametric and Dunn's post hoc pairwise comparison tests ($p < 0.05$) are annotated with an asterisk above the boxplots.

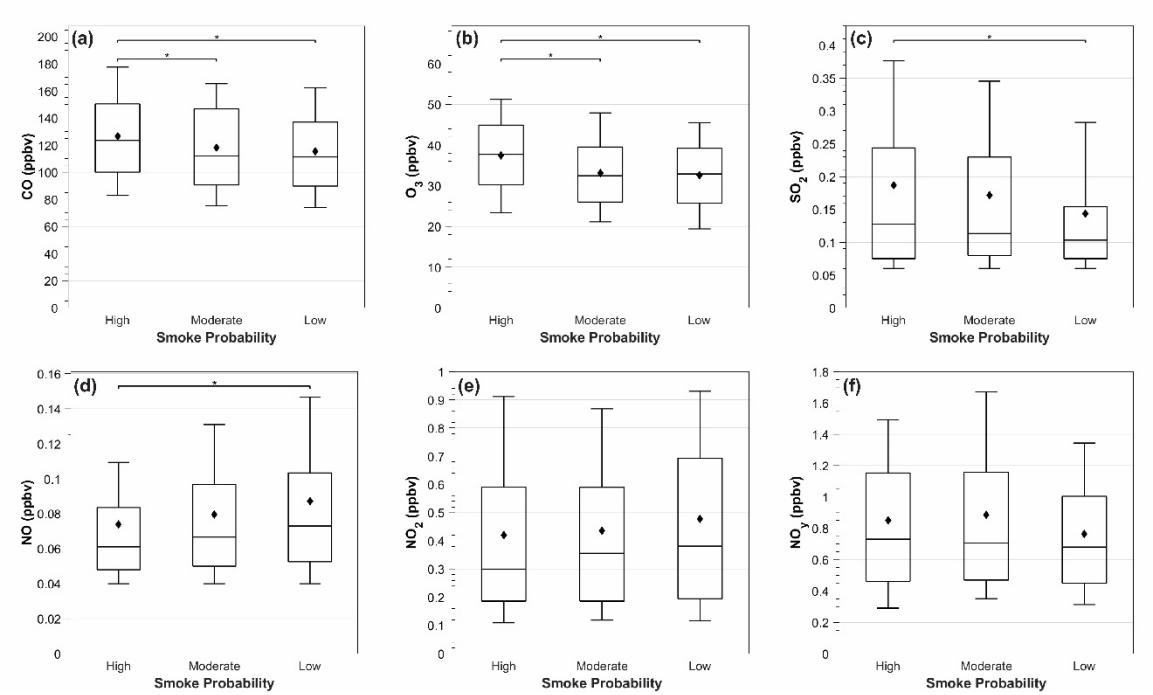


Figure S3. Boxplot distributions for atmospheric trace gases levels: (a) carbon monoxide (CO), (b) ozone (O_3), (c) sulfur dioxide (SO_2), (d) nitric oxide (NO), (e) nitrogen dioxide (NO_2), and (f) total nitrogen oxides (NO_y) per category of smoke influence probability (high, moderate, and low). Boxplots represent the 25th, 50th, and 75th percentiles, with whiskers representing the 10th and 90th percentiles. Average concentrations per smoke category are marked as diamonds. Significant differences in the distribution that met both the Kruskal-Wallis non-parametric and Dunn's post hoc pairwise comparison tests ($p < 0.05$) are annotated with an asterisk above the boxplots.

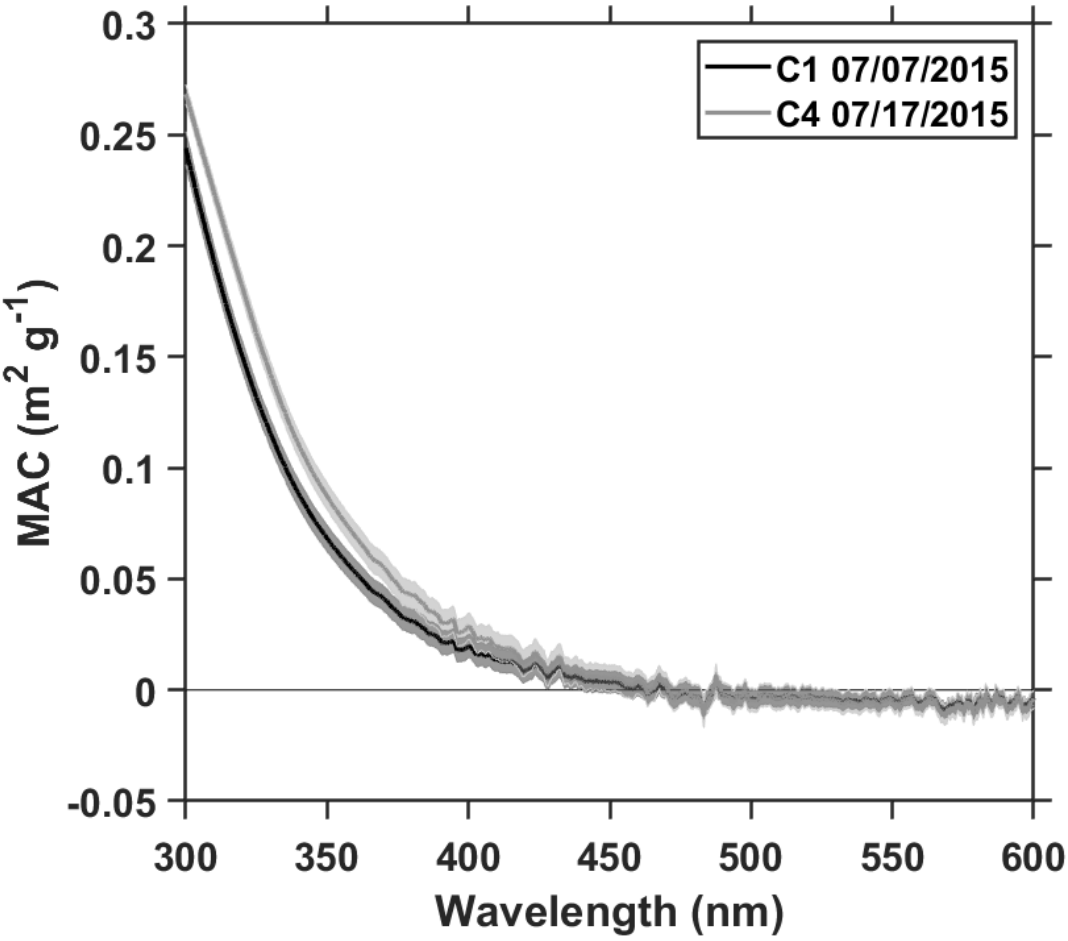


Figure S4. UV-visible absorbance spectra plotted as the mass absorption coefficient (MAC) versus wavelength for two smoke-influenced cloud water samples (C1 and C4).

Table S1. Minimum, maximum, median, and average concentrations with 95% confidence intervals (CI) for measured inorganic ion concentrations, liquid water content (LWC), pH, and total organic carbon (TOC) concentrations for cloud water collected at Whiteface Mountain Observatory with samples classified by probability of smoke influence (high, moderate, low). *n* refers to the number of cloud water samples in each smoke classification. Kruskal-Wallis p-value and the following Dunn's post hoc test are reported for each classification comparison.

	High Smoke Probability (n = 340)					Moderate Smoke Probability (n = 179)					Low Smoke Probability (n = 819)					Kruskal-Wallis p-value	Dunn's post test
	Min	Max	Median	Mean	95% CI	Min	Max	Median	Mean	95% CI	Min	Max	Median	Mean	95% CI		
SO_4^{2-} (μM)	1	580	27	59	8	1	317	10	48	10	bdl	363	17	37	3	$< 10^{-6}$	High vs Moderate ($p = 0.35$) High vs Low ($p < 10^{-6}$) Moderate vs Low ($p = 0.05$)
NO_3^- (μM)	1	1140	30	70	10	2	690	10	60	10	0.4	1127	20	39	4	$< 10^{-7}$	High vs Moderate ($p = 0.25$) High vs Low ($p < 10^{-7}$) Moderate vs Low ($p = 0.04$)
Cl^- (μM)	0.2	44.1	2	4.3	0.7	0.1	45	1	5	1	0.1	209.9	1.4	3.4	0.6	$< 10^{-5}$	High vs Moderate ($p = 0.91$) High vs Low ($p < 10^{-5}$) Moderate vs Low ($p = 0.01$)
Ca^{2+} (μM)	bdl	541	6	18	5	bdl	179	4	15	4	bdl	743	3	8	2	$< 10^{-14}$	High vs Moderate ($p = 1.00$) High vs Low ($p < 10^{-11}$) Moderate vs Low ($p < 10^{-6}$)
Mg^{2+} (μM)	bdl	86.3	1.9	4.4	0.9	bdl	45.4	0.9	4	0.9	bdl	55.6	1	2.1	0.3	$< 10^{-17}$	High vs Moderate ($p = 0.99$) High vs Low ($p < 10^{-14}$) Moderate vs Low ($p < 10^{-8}$)
Na^+ (μM)	0.1	52.9	1	3.3	0.7	0.1	49	1	4	1	bdl	230.6	0.7	3.2	0.8	$< 10^{-3}$	High vs Moderate ($p = 1.00$) High vs Low ($p < 10^{-2}$) Moderate vs Low ($p = 0.02$)
K^+ (μM)	bdl	36.6	1.3	2.5	0.4	bdl	24	0.4	1.9	0.4	bdl	43.6	0.7	1.5	0.2	$< 10^{-16}$	High vs Moderate ($p = 0.16$) High vs Low ($p < 10^{-15}$) Moderate vs Low ($p < 10^{-4}$)
NH_4^+ (μM)	2	1540	60	140	20	2	690	20	100	20	bdl	749	35	72	7	$< 10^{-9}$	High vs Moderate ($p = 0.13$) High vs Low ($p < 10^{-9}$) Moderate vs Low ($p = 0.01$)
LWC (g/m^3)	0.03	1.73	0.54	0.56	0.03	0.05	3.24	0.44	0.5	0.05	0.01	3.23	0.56	0.59	0.03	$< 10^{-3}$	High vs Moderate ($p = 0.02$) High vs Low ($p = 0.56$) Moderate vs Low ($p < 10^{-3}$)
pH	3.6	6.64	4.64	4.69	0.06	3.46	6.34	4.66	4.68	0.08	3.47	6.49	4.67	4.72	0.04	0.42	N/A
TOC (mM)	0.04	2.39	0.33	0.44	0.05	0.03	1.35	0.28	0.36	0.05	bdl	2.43	0.21	0.28	0.02	$< 10^{-12}$	High vs Moderate ($p = 0.35$) High vs Low ($p < 10^{-12}$) Moderate vs Low ($p < 10^{-3}$)

Table S2. Five case study cloud water samples. Smoke conditions were classified based on when the NOAA HYSPLIT 72 h backward air mass trajectory overlapped with smoke from the HMS Fire and Smoke Product. Insoluble particle concentrations and mode particle diameters measured by nanoparticle tracking analysis (NTA), mass absorption coefficients between 360 – 370 nm (MAC_{365}) and absorption Ångström exponent (AAE) for selected case study samples listed. Standard errors are shown when possible.

Sample ID	Smoke Probability	Sampling Start Time	Hour Trajectory Started Overlapping with Smoke (h)	Total Hours Trajectory Overlapped with Smoke (h)	Was There Precipitation Along Back Trajectory	Total Hours Trajectory Height < MLD (h)	Insoluble Total Particle Conc. (# cm^{-3})	Insoluble Particle Peak Diameter Mode (nm)	MAC_{365} (m^2 g^{-1})	AAE
C1	High	7/7/2015 18:00	0	39	Yes	10	3 E+8 ± 2 E+7	135 ± 6	0.046 ± 0.001	9
C2	High	8/16/2014 18:00	2	60	No	1	6 E+7 ± 3 E+6	185 ± 14	N/A	N/A
C3	High	8/18/2014 6:00	0	13	Yes	0	N/A	N/A	N/A	N/A
C4	Low	7/17/2015 18:00	NaN	NaN	Yes	9	1 E+8 ± 6 E+6	142 ± 9	0.061 ± 0.001	8
C5	Low	7/21/2015 18:00	NaN	NaN	Yes	0	1 E+8 ± 4 E+6	247 ± 20	N/A	N/A

Table S3. Average concentrations for organic compounds measured by various chromatography techniques for selected smoke-influenced cloud water samples collected at the Whiteface Mountain Observatory (Table S2). Values below the limits of detection are marked as "bdl". Measurement uncertainty for each species is estimated to be 10%.

Sample ID	Levoglucosan (μM)	Mannosan (μM)	Galactosan (μM)	Galactose (μM)	Glucose (μM)	Mannose (μM)	Glycerol (μM)	Inositol (μM)	Threitol (μM)	Mannitol (μM)	Arabinose (μM)	Xylose (μM)	Acetate (μM)	Proponiate (μM)	Formate (μM)	MSA (μM)	Glutrate (μM)	Succinate (μM)	Malonate (μM)	Maleate (μM)	Oxalate (μM)	Total Concentration of Carbohydrates (μM C)
C1	0.04	bdl	0.005	0.009	0.12	0.020	0.3	0.075	bdl	0.05	0.028	bdl	0.1	bdl	0.2	bdl	0.61	2.1	0.07	bdl	2.3	19 ± 1
C2	0.02	0.02	0.003	bdl	0.02	bdl	0.8	0.007	bdl	0.03	bdl	0.0001	1.2	0.02	1.2	0.2	0.03	0.1	0.03	0.03	0.4	8.4 ± 0.4
C3	0.09	0.12	0.028	0.010	0.40	0.001	8.4	0.389	bdl	0.21	0.023	0.0008	15.5	bdl	6.9	0.1	1.57	0.5	0.37	0.16	1.7	86 ± 4
C4	0.04	bdl	0.003	0.007	0.07	0.007	0.5	0.144	bdl	0.07	0.013	bdl	0.5	0.07	0.2	bdl	0.18	0.8	0.12	bdl	1.2	11.9 ± 0.5
C5	0.07	0.12	0.005	0.004	0.07	bdl	9.7	0.364	bdl	0.07	0.004	bdl	1.3	bdl	0.6	2.7	0.03	0.1	0.16	0.08	0.8	42 ± 3